



Magnetic Properties of the Dilute Magnetic Semiconductor $\text{Zn}_{1-x}\text{Co}_x\text{O}$ Nanoparticles

Prissana Robkhob¹ · I. Ming Tang² · Sirikanjana Thongmee¹

Received: 16 January 2019 / Accepted: 5 May 2019 / Published online: 23 May 2019
© Springer Science+Business Media, LLC, part of Springer Nature 2019

Abstract

The magnetic properties of the dilute magnetic semiconductor (DMS) are due the existence of two competing interactions, a direct ferromagnetic interaction and an indirect antiferromagnetic interaction. This is well established in the $\text{Zn}_{1-x}\text{Mn}_x\text{O}$ DMS, but is controversy in the $\text{Zn}_{1-x}\text{Co}_x\text{O}$ DMS. To gain insights, a series of Co-substituted ZnO NRs ($x = 0, 0.01, 0.02, 0.03, 0.04,$ and 0.05) have been fabricated using a low-temperature hydrothermal method. The magnetization of these Co-doped ZnO NPs was measured with a vibrating sample magneto-meter. Expressing the magnetization results in units of Bohr magnetons per Co ions, it is found that the ferromagnetic contributions become more dominant as more magnetic Co ions are doped into the ZnO NPs. X-ray diffraction, energy dispersive X-ray, scanning electron microscopy, and photoluminescence measurements were done to characterize the Co:ZnO NPs.

Keywords Dilute magnetic semiconductor (DMS) · ZnO nanorods · Co impurities · Magnetic moments · Competing interactions

1 Introduction

The discovery of ferromagnetism in the semiconductor EuO [1] excited the technology world since the new stratagem for advanced information technology (spintronic) is to utilize both the charge and spin of the electrons stored on a bit. To detect the presence of a stored spin on the bit but also the direction of the spin, that will need spin-polarized currents. One way to obtain such a current is to use a magnetic semiconductor. Passing a current through such a semiconductor, the spin up component of the current would be shifted to a lower energy while the spin down component would be shifted to a higher energy resulting in the current being split into a spin down current and a spin up current. The presence of an energy gap would prevent the passage of the one component having energies lower than the energy gap. A device in which this occurred was made by Schmehl et al. [2]. The

shortcoming of EuO is that the Curie temperature (T_C) of EuO is below room temperature.

Furdyna [3] found that doping various semiconductors with Mn ions made them paramagnetic with the possibility of them becoming ferromagnetic at some temperature. These doped semiconductors have been given the name “dilute magnetic semiconductors” (DMS). Ohno et al. [4] found that ferromagnetic ordering of 60 K could be achieved in the semiconductor GaAs by doping 3% Mn into the GaAs. Dietl et al. [5] modified the Zener theory [6] to predict above room temperature T_C 's in various III–V and II–VI compound semiconductors when doped with Mn impurities. Coey, Venkatesan, and Fitzgerald [7] predicted the T_C 's of different II–VI semiconductors doped with other magnetic transition metal ions. Ventatesan et al. [8] measured the magnetic moments in ZnO thin films doped with 5% Sc, Ti, V, Fe, Co, Ni, Cr, Mn, and Cu. They found that the highest magnetic moments in these DMS films occurred in the Co-doped ZnO films. Anghej et al. [9] measured the saturation magnetizations of ZnO nanoparticles doped with 5% (and 2%) Cr, Mn, Fe, Co, or Ni. They found however that the highest saturation magnetization occurred in the Fe-doped ZnO nanoparticles.

Both Dietl et al. [5] and Coey, Venkatesan, and Fitzgerald [7] assumed that the ferromagnetic exchange was mediated by the carriers in the spin-orbit impurity band formed by overlapping bound magnetic polarons (BMPs). The BMPs for the

✉ Sirikanjana Thongmee
fscisjn@ku.ac.th

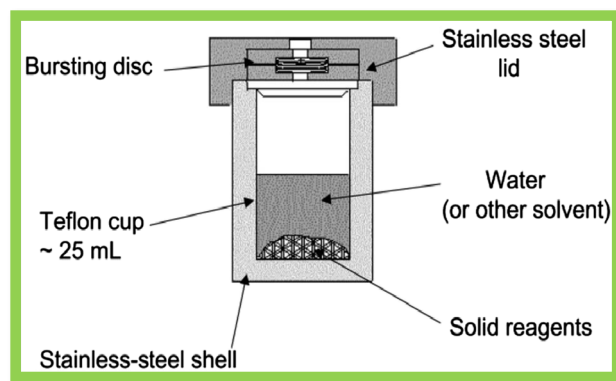
¹ Department of Physics, Faculty of Science, Kesarsart University, Bangkok 10900, Thailand

² Department of Mathematics, Faculty of Science, King Mongkut's University of Technology Thonburi, Bangkok 10140, Thailand

case of Mn doping are created by the Mn^{2+} ion and a singly charged oxygen vacancy defect (V_{O}^+). The ferromagnetic exchange arises from the *sp-d* interactions between the shallow donor carriers from the oxygen defects and the *d* electrons of the impurity ion. In ref. [5], the carriers were taken to be holes while in ref. [7], they were taken to be electrons. In either case, the carriers would be spin-polarized. These same spin-polarized carriers would then overlap the *d* electrons of a neighboring impurity ion causing a parallel alignment of the spins of the two TM ions. Large magnetic moments occur when there is a large density of the d^{\uparrow} or d^{\downarrow} electrons at the Fermi level (see Fig. 4 in ref. [7]). Other oxygen defect in the system could also form a second BMP with another TM impurity ion. There would be an interaction between these two BMPs and it would be an indirect TM-O-TM interaction which would be antiferromagnetic one [10]. The direct TM-TM interaction would be ferromagnetic. The magnetic state of VMS would be the net result of two competing interactions, i.e., net interaction in the Heisenberg Hamiltonian for the VMS.

Recently, Thongjamroon et al. [11] looked at the effects of replacing some of the Zn^{2+} ions in ZnO nanoparticles with the magnetic Mn^{2+} ion. It was observed that the magnetic moments of the Mn^{2+} ions decreased as more of these TM ions were substituted into the NPs. This decrease was observed when the magnetization was expressed in units of Bohr magnetons per Mn^{2+} ion. An increase would be seen if the saturation magnetization was expressed in emu/g since the gm term refers to the whole mass of $\text{Zn}_{1-x}\text{Mn}_x\text{O}$ NPs including the masses of the nonmagnetic Zn and O, while the emu depends only on the amount of the Mn ions in the NPs. According to Dietl et al., and Coey, Venkatesan, and Fitzgerald, the exchange interaction is the result of the competition between the ferromagnetic interaction and the antiferromagnetic interaction. Since the average distances between the dopant magnetic ions in the wurtzite structures of the doped ZnO NPs decrease as more dopant is substituted in, the two interactions (the direct TM-TM and the indirect TM-O-TM) would change in different fashions, resulting in the net exchange interaction being dependent on the level of substitution.

The existence of RT ferromagnetism in lightly doped Co:ZnO NRs is controversial. In the first publication on RT ferromagnetism in this DMS, Uede et al. [12] stated that “the repro-ducebility of the method was poor (less than 10%).” The range of the different results has been given by Ney [13]. Part of the reason for the low reproducibility of the results could be the role of defects needed for ferromagnetic order [14]. Martinez et al. [15] reported that Co-doped ZnO NPs prepared at different pressures had quite different magnetic behaviors. Those prepared at low pressures were ferromagnetic at low temperatures, while those prepared at high pressures were paramagnetic. Balti et al. [16] reported that their Co-doped ZnO NPs were paramagnetic at 5 K. Franco



Scheme 1 Schematic representation of hydrothermal process

et al. [17] found that different amounts of the Co^{2+} ions were coupled at different temperatures: at 5 K, 26% of the Co^{2+} ions were FM coupled; at 30 K, 67% were FM coupled, but above 50 K, most of the Co^{2+} ions were PM or AFM coupled. These latter results should be compared to the initial result reports [5, 7, 8–9] of ferromagnetism in the TM-doped ZnO NPs.

To obtain more insights into the room temperature ferromagnetism in the VMS doped with magnetic impurities, we have chosen to study the change in the magnetic properties of the Co-doped ZnO NPs as more Co is substituted in. We have fabricated Co-doped ZnO NPs of stoichiometric composition $\text{Zn}_{1-x}\text{Co}_x\text{O}$ ($x = 0.00, 0.01, 0.02, 0.03, 0.04, \text{ and } 0.05$) using the low-temperature hydrothermal method. We carried out X-ray diffraction (XRD) studies to determine the crystal structure. Scanning electron microscopy (SEM) and energy dispersive X-ray (EDX) were done to observe and determine the morphologies and actual chemical contents of the various Co-doped ZnO NPs. Photoluminescence studies were carried out on the ZnO and the Co-doped ZnO NPs to gain information on the types of defects existing in the NPs. The effects of the Co doping on the energy gaps of the semiconductors are seen using a UV-visible light (UV-vis) spectrometer. Finally, a vibrating sample magnetometer (VSM) was used to measure the magnetic properties of the Co-doped ZnO NPs.

2 Experimental Details

The hydrothermal method was used to synthesis the Co-doped ZnO nanoparticles. This method is cost-effective and simple. It employs hot water and high vapor pressure. In the solid-state reaction method, the two metal oxides would be mixed together and heated to over 1000 °C in order for the transition metal ions to be able to diffuse in the solid until they reached each other and reacted. In the hydrothermal method, the reaction is a chemical process and the ions are able to come into contact with each other more easily. The higher room temperature used in the autoclave allows the oxide compounds to disassociate into their ion constitutes since the solubility

increases with temperature. The high pressure is needed so that the solvent does not evaporate. At the high temperature (180 °C), the ions will move faster. After the nanoparticles are formed, the solution is cooled down to room temperature. The solubility drops and the nanoparticles precipitate out.

Aqueous solutions of zinc nitrate hexahydrate ($\text{Zn}(\text{NO}_3)_2 \cdot 6\text{H}_2\text{O}$) with 1, 2, 3, 4, and 5 mol% cobalt nitrate hexahydrate ($\text{Mg}(\text{NO}_3)_2 \cdot 6\text{H}_2\text{O}$) were separately dissolved in 50 ml of water and each of these mixtures was stirred for 30 min. Then, 0.029 g of ethylene diamine tetra acetic acid EDTA was added to each mixture and stirred for another 20–30 min. Finally, ammonia was added to each mixture under continuous stirring conditions until the pH of each mixture reached 10. The chemicals in each mixture were enough to produce the chemical product $\text{Zn}_{1-x}\text{Co}_x\text{O}$ ($x = 0.00, 0.01, 0.02, 0.03, 0.04,$ and 0.05). Each of the resulting mixture was individually placed inside a Teflon-lined autoclave and heated to 180 °C inside an oven for 20 h. The autoclave was then removed from the oven and allowed to cool down in air to room temperature. The nanostructure deposits inside each of the cooled solutions were washed several times with distilled water and dried in an oven at 110 °C for 3 h.

3 Results and Discussion

3.1 X-ray Diffraction

The crystal structures of the six samples are obtained from the XRD patterns that are shown in Fig. 1. These XRD patterns exhibit the diffraction peaks in all the samples between $2\theta = 20$ – 80° . The peaks of the pure ZnO (shown in Fig. 1(a)) are the reflections from the (110), (002), (101), (102), (110), and (103) planes, respectively. These belong to the hexagonal wurtzite structure.

The XRD patterns for the Co-doped ZnO NPs are shown in Fig. 1(b)–(f). As we see, the diffraction peaks appear at similar positions indicating that the Co-doped ZnO NPs still have the wurtzite structure with no impurity (or secondary) phase appearing. The lattice parameters are calculated using the standard formulas from the Miller indices for the wurtzite structure. The values of the lattice parameters a and c and the ratio a/c of the six NPs are listed in Table 1. The ionic radii of the two TM ions, Zn^{2+} and Co^{2+} , have been reported to be 0.74 nm and 0.72 nm, respectively [18]. If the substitution of the Zn^{2+} ions by the Co^{2+} is the only thing occurring, then the lattice parameters should systematically decrease. But as we see, this systematic decrease is not observed. Instead, we observe initial increases as the Co^{2+} ions are first doped in, followed by decreases (and then increases as more Zn^{2+} are replaced). In general, the lattice parameters decrease as more Co replaces the Zn ions as shown in Table 1. The

observed behaviors must be due to something else which is accompanying the substitution of the Zn by the Co.

3.2 Photoluminescence Studies

As pointed out in the Section 1, the magnetic behaviors in the VMS could be due to the defects in the crystal structures of the nanorods when they are made by the hydrothermal process. The non-monotonic behavior of the lattice parameters could be due to the formation of the defects. Annealing the NRs at high temperatures would remove some of the defects. One method to identify the defects is to look at the photoluminescence spectra (PL) of the NPs. A typical PL spectrum of ZnO nanorods consists of two peaks. The sharp peak at 378 nm is due to the emission of a UV radiation resulting from the transition of an excited electron in the conduction band to an empty state in the valence band.

The empty state in the valence band was created when an electron in the valence band was excited to an empty state in the conduction band. In the ZnO nanoparticles, the excited e^- and the hole (h^+) left behind can form into an electron-hole (e^-/h^+) pair called an exciton. The 378 nm peak corresponds to the energy difference between the energy levels of the excited state and the ground state minus the binding energy of the exciton. The broad band between 400 and 650 nm originates from transitions between energy levels created when defects in the crystal structures of the ZnO are formed. The defects can be the oxygen vacancies, V_{O} ; oxygen interstitials, O_i ; singly ionized oxygen interstitial, O^-_i ; zinc vacancies, V_{Zn} ; zinc interstitial, Zn_i ; or excess oxygen on the surface of the NPs. The radiation

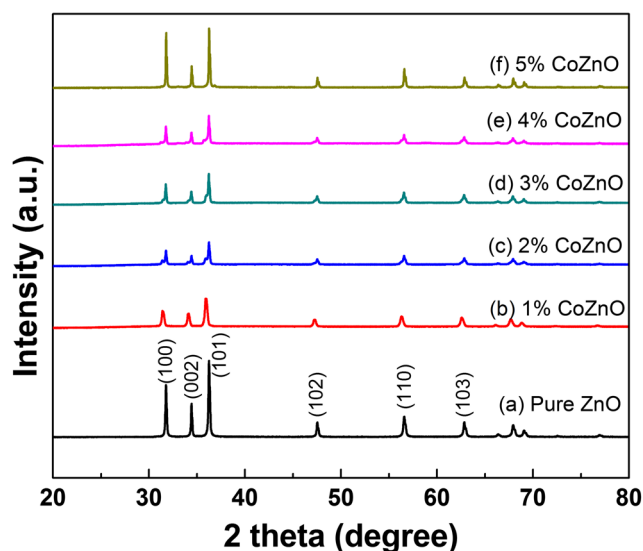


Fig. 1 XRD patterns of ZnO and Co-doped ZnO. (a) Pure ZnO, (b) 1 wt%, (c) 2 wt%, (d) 3 wt%, (e) 4 wt%, and (f) 5 wt% of Co doping, respectively. All the peaks could be indexed to the hexagonal wurtzite structure of ZnO NPs with no impurity phases seen

Table 1 Lattice parameters of the Co-doped ZnO nanocomposites

| Samples | Lattice parameter | | |
|----------|-------------------|---------|--------|
| | $a = b$ (Å) | c (Å) | a/c |
| Pure ZnO | 3.2463 | 5.2012 | 1.6022 |
| Co 1 wt% | 3.2813 | 5.2494 | 1.5998 |
| Co 2 wt% | 3.2485 | 5.2012 | 1.6011 |
| Co 3 wt% | 3.2506 | 5.2075 | 1.6020 |
| Co 4 wt% | 3.2485 | 5.2044 | 1.6021 |
| Co 5 wt% | 3.2463 | 5.1980 | 1.6012 |

emitted when there is transition between these levels and the ground states, between the excited states, or between the defect states. The 427 nm (blue) radiation in PL emissions is connected to the Zn_i defects; the 485 nm (green), singly ionized V^+_{O} vacancy; the 544 nm, O_i ; 560 nm, O^-_i ; the 600–640 nm, V_{O} ; and the blue-green radiation from the surface defects. By observing the changes in the intensities at different wavelengths, the nature of the defects in the ZnO NPs can be determined [19].

In Fig. 2(b) and (c), we see that visible light PL spectrum of the pure ZnO NPs is suppressed in the spectrum of

the Co-doped NPs, especially between 425 nm and 525 nm. This could mean that the defects Zn_i are suppressed by the replacement of Zn by Co ions. The dips in the PL spectrums around 550 nm in most of the Co-doped NRs could be due to the additional formation of oxygen interstitials, O_i or O^-_i , as more Co^{2+} ions replace the Zn^{2+} ions. Looking more closely at Fig. 2(c), we see three peaks at approximately 540, 560, and 640 nm in the 1% Co-doped NRs. These peaks are signs of defects due to O_i , V^+_{O} , or V_{O} , respectively. Of special interest are the 560 nm PL signals in the 3%, 4%, and 5% Co-doped NP spectrums, the intensities tend to increase, meaning that the formation of additional singly ionized oxygen interstitials as more Co ions replace the Zn ions at these doping levels.

3.3 Energy Dispersive X-ray Studies

The oxygen ion content in the different NRs can be determined from the energy dispersive X-ray (EDX) studies done on the NRs. These studies have been done since the chemical formula of the different nanoparticles given as $Zn_{1-x}Co_xO$ with $x = 0.0, 0.01, 0.02, 0.03, 0.04,$ and 0.05 give the stoichiometric amounts of the Zn and Co ions dissolved into the aqueous solutions. We need to know

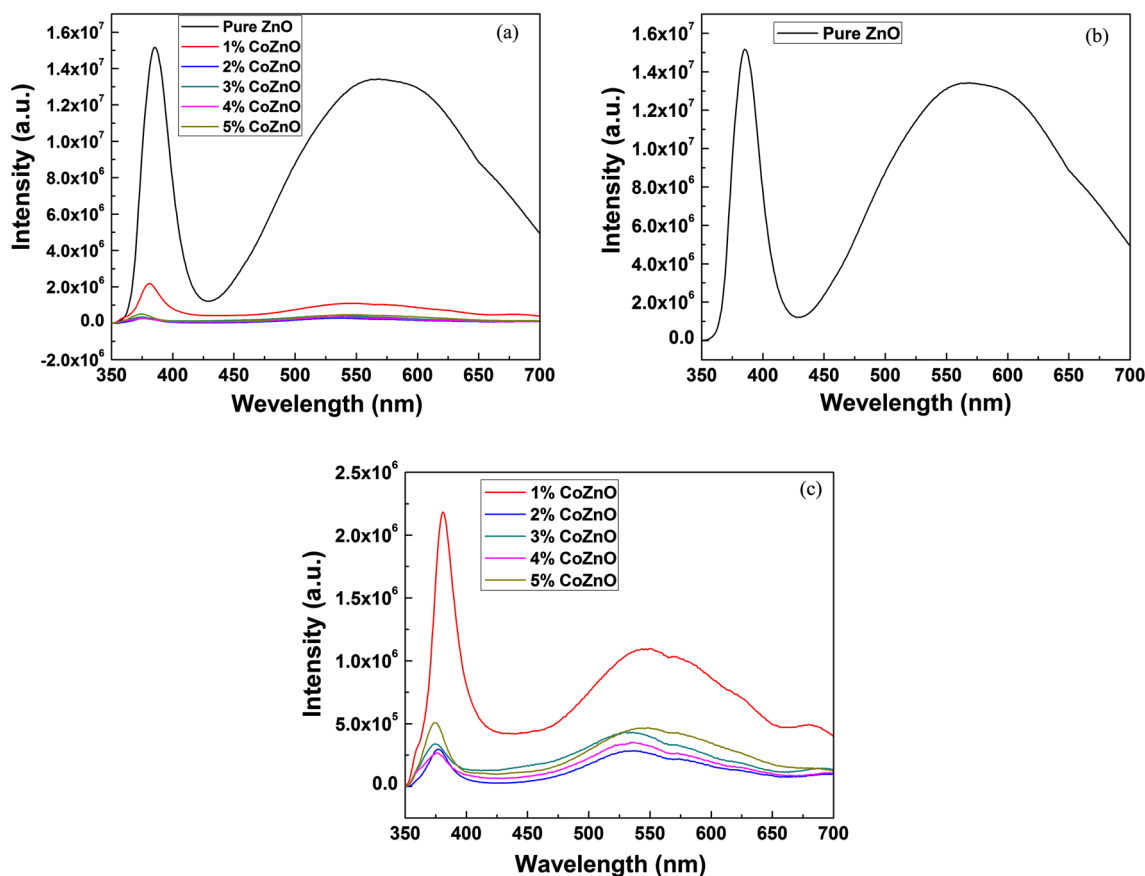


Fig. 2 Photoluminescence spectrums at room temperature. (a) PL spectrums of undoped ZnO and all the Co-doped ZnO NRs. (b) PL spectrum of the undoped ZnO NRs. (c) Spectrums of only the doped NRs. All the exciton peaks exhibit a red shift of the NBE peaks

the amounts of Zn and Co which actually entered into the wurtzite structure. These can be determined from the energy dispersive X-ray (EDX) spectrum along with the amount of oxygen ions. Figure 3 shows the EDX spectrum of the 5% cobalt-doped NPs. From this spectrum and the spectrums for other doped ZnO NPs, we obtain the amounts of Zn, Co, and O in the Co-doped NPs. These are listed in second three sets of lines in the Table 2. These numbers can be used to calculate the actual chemical formula of the nanoparticles. The actual compositions of the nanorods are given in Table 2.

3.4 Scanning Electron Microscopy Studies

In several places in this paper, we have referred to the ZnO nanoparticle as nanorods. To show that this is true, we now present the SEM images of the pure ZnO NRs (Fig. 4(a)) and the 3% Co-doped ZnO NPs (Fig. 4(b)). The SEM images of the other Co-doped ZnO NRs are similar and so are not shown. The morphologies of pure ZnO NP and others show that the shapes of the Co-doped ZnO NPs are of hexagonal rods. This is consistent with the XRD results. When the Co is substituted in, the SEM images (Fig. 4(b)) are still those of nanorods but with shorter c-axis and larger diameters as more Co replaces the Zn ions in the hexagonal wurtzite structure. The images also show that clustering of the of the nanorods increases as more Co are doped in.

3.5 UV-Vis Absorption Spectrum

Throughout this paper, we have called ZnO a semiconductor. A semiconductor is characterized by an electronic band gap (energy gap). The energy gap is slightly larger than the optical band gap since the measurement of the first involves the overcoming of some Coulomb interactions not present in the measurement of the second. Since the difference is small and the optical measurements are easier to do, the energy gap of a semiconductor is usually measured using the optical measurements. These are usually done with a UV-vis light

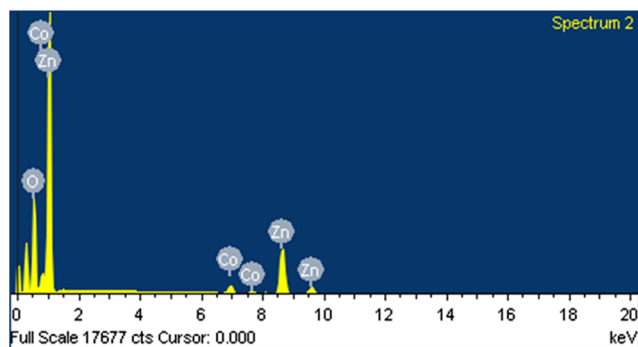


Fig. 3 EDX spectrum of 5% Co-doped ZnO nanoparticle. The EDX spectrums of the other Co-doped ZnO NPs are similar to the ones shown. The information from these EDX spectrums is given in Table 2

Table 2 Atomic percentage of pure ZnO and Co-doped ZnO nanocomposites

| Samples | Zn atomic % | O atomic % | Co atomic % |
|----------|-------------|------------|-------------|
| Pure | 41.29 | 58.71 | – |
| Co 1 wt% | 46.70 | 52.85 | 0.45 |
| Co 2 wt% | 35.71 | 63.49 | 0.80 |
| Co 3 wt% | 29.68 | 68.52 | 1.80 |
| Co 4 wt% | 31.72 | 66.01 | 2.27 |
| Co 5 wt% | 29.90 | 67.53 | 2.57 |

spectrometer. The optical absorption spectrums of ZnO and Co-doped ZnO are shown in Fig. 5(a). From the spectrums in this figure, we can extract the information needed to construct the Tauc plots which are the plots of $(\alpha hv)^2$ as function of hv . These are shown on Fig. 5(b).

The values of the optical band gap can be obtained by the linear extrapolation of the linear portion of the Tauc relations given below [20].

$$(\alpha hv)^2 = A(hv - E_g) \quad (1)$$

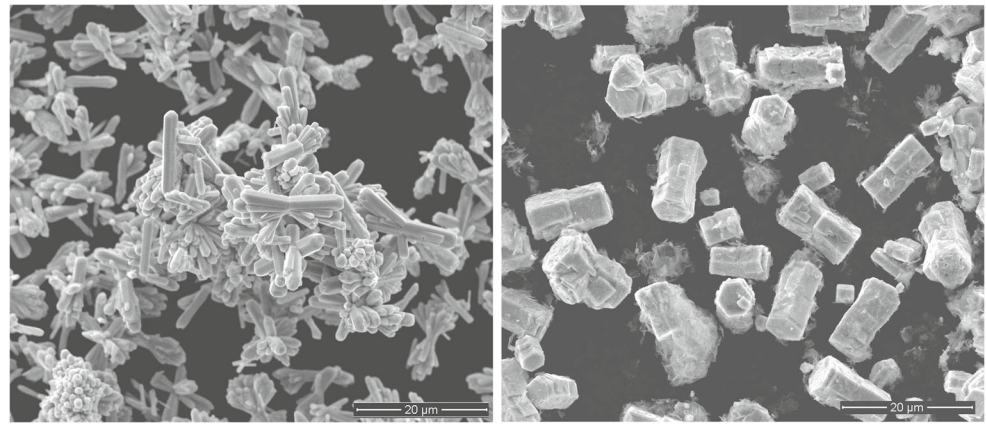
where α is the absorption coefficient, hv is the photon energy, A is a constant, and E_g is the optical band gap. The plots of $(\alpha hv)^2$ as function of hv for all samples are shown in Fig. 5(b). The value of energy band gap of pure ZnO is 3.218 eV and the energy band gap of the doped ZnO semiconductors decreases to 2.679 eV after the Co doping increase. The values of the energy gap in each semiconductor appear in the Table 3. The narrowing of the energy gaps is due to the increased perturbations (due to increased replacement of the Zn ions by the Co ions) acting on the valence band and conduction band electrons. The increases in the energy states of two electrons (one in the valence band and the other in the conduction band) due to the perturbation are not the same and so the difference between the two changes and we get a narrowing of the gap (seen in the Table 3).

3.6 Vibrating Sample Magnetometer Studies

Most studies of the magnetization of materials express their results in units of emu/g or emu/cm³. For studies on the effects of substitution of magnetic impurities into host systems, the use of these units could lead to false conclusion of the trend of the effects since the emu depends on the magnetic component of the particle, while the mass and volume of particle depend on all the components of the particle. Expressing the results as number of Bohr magnetons per magnetic ions provides a better picture of the magnetism in the system.

Figure 6 showed the hysteresis loops of the pure ZnO NR and the 3% Co-doped NRs. The hysteresis loops for the other Co-doped ZnO NRs are similar in shape to those of the 3%

Fig. 4 SEM images of pure ZnO and 3% Co-doped ZnO. (a) SEM image of pure ZnO NPs. (b) SEM images of 3% Co-doped NPs. The SEM images of the other Co-doped NPs are similar and they show the shapes of the NPs are those of hexagonal shape nanorods



Co-doped NRs. In Fig. 6(a), which is for the pure ZnO NRs, we have subtracted the diamagnetic signals (the linear portion of the loop at high H fields). In the Fig. 6(b), this was not done. From the hysteresis loops of all of the Co-doped ZnO NPs, we extracted the values of the values the field H needed to flip the spin as the field strength increased or decreased, $H_{C\uparrow}$ and $H_{C\downarrow}$. As we see, $H_{C\uparrow}$ of left hand side (LHS) is the intersection hysteresis loop with the $M = 0$ axis, while $H_{C\downarrow}$ is the intersection so the right hand side (RHS) of the hysteresis loop. The average of these two coercive fields, the saturation magnetization M_S in units of emu/g, and the values in units are listed in the Table 4. To carry out this recalculations, the actual amounts of Co ions in gram of the nanocomposites were taken to be the values determined by the EDX measurements (Table 2).

In Fig. 7, we have plotted the values of the saturation magnetization vs. actual percentage of Co incorporated into the NPs.

This is different from the behavior of the saturation magnetization when Mn ions replaced the Zn ions in the ZnO NRs [11]. Thongjamroon et al. reported that as the amount of Mn increased from 1.39 to 2.24 to 3.68%, the saturation magnetization decreased from 2.51 to 2.23 to $2.2.34 \times 10^{-2} \mu_B/\text{Mn}$ ion. To account for their observed behavior, Thongjamroon et al. proposed that the net exchange interaction decreases as

more Mn is doped into the hexagonal wurtzite structure of ZnO NRs.

To understand the differences between the two sets of results, plotted in Fig. 7 of this paper and Fig. 5 of ref. 11, we first note that magnetic interaction (Heisenberg Hamiltonian) in the dilute magnetic semiconductor $\text{Zn}_{1-c}\text{X}_c\text{O}$ (where X is a magnetic TM ion, Co or Mn) is

$$-\sum_{ij} J_{ij} \bar{S}_i \cdot S_j c_i c_j \quad (2)$$

where c_i is the site occupancy operator introduced by Edwards [21] ($c_i = 1$ if the site i is occupied and is equal to “0” if not occupied). The operator also has the property that $(c_i)^n = c_i$; \bar{S}_i , the spin operator for the cobalt ion located at the site i and J_{ij} is the net exchange interaction between a Co ion located at site i and another Co ion located at site j . The standard assumption is $J_{ij} = \pm |J|$ if i and j are nearest neighbors. The positive sign is used if the exchange interaction is ferromagnetic, while the negative sign is used if the interaction is antiferromagnetic. To proceed further, we convert the two spin interactions into a one spin interaction by making the Hartree-Fock approximation $\bar{A}_i \cdot \bar{B}_j = \bar{A}_i \langle B \rangle + \langle A \rangle \bar{B}_j$ where \bar{A}_i and \bar{B}_j are the spin operators at sites i and j and $\langle \rangle$ denotes the average (over all possible sites) and the thermo average (as such $\langle \rangle$

Fig. 5 UV-vis optical absorption studies of the pure ZnO and Co-doped ZnO NRs. (a) UV-vis optical absorption spectrum of each doped NRs. (b) Tauc plots of the UV-vis optical absorptions of each Co-doped ZnO NRs

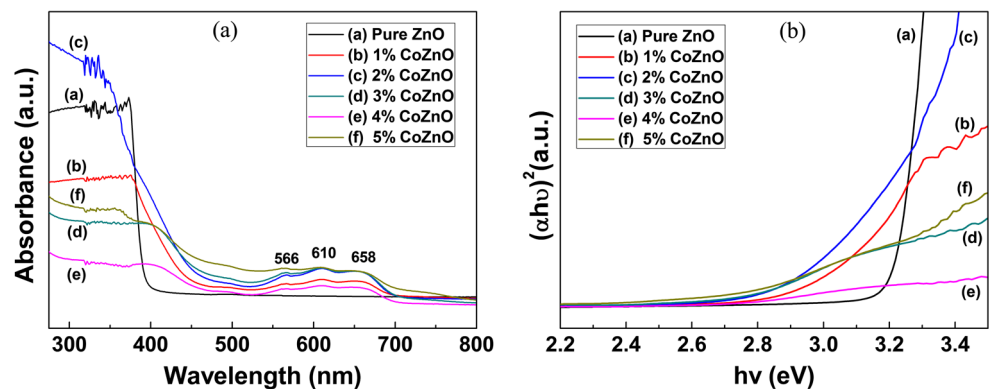


Table 3 Energy band gap of pure ZnO and Co-doped ZnO nanocomposites

| Chemical formula | Energy band gap (eV) |
|--|----------------------|
| ZnO | 3.218 |
| Co _{0.009} Zn _{0.934} O _{1.057} | 3.039 |
| Co _{0.016} Zn _{0.714} O _{1.269} | 2.938 |
| Co _{0.036} Zn _{0.594} O _{1.370} | 2.720 |
| Co _{0.045} Zn _{0.634} O _{1.320} | 2.687 |
| Co _{0.051} Zn _{0.598} O _{1.351} | 2.679 |

does not depend on any particular site). The exchange interaction now becomes

$$-2\sum_{ij} J_{ij} S_i < S > c_i c_j \tag{3}$$

where J_{ij} is assumed for i and j being nearest neighbors to negative if the system is ferromagnetic and the positive if the system is antiferromagnetic. Noting that only the site occupancy operator depends on j , the summation over j can easily be done. Doing this, the magnetic interaction in Zn_{1-c}Co_cO is reduced to

$$\mp 2c |J| \sum_i S_i c_i \tag{4}$$

where the positive sign is used if the system is ferromagnetic and the negative sign is used if the system is antiferromagnetic. The above interaction now becomes the perturbation to the host ZnO system. The perturbative correction can be easily determined from Dyson’s equation applied to the configuration average of the resolvent $1/(E - V_j)$. The n th order correction would be the sum of the irreducible diagram involving n interactions multiplied by the cumulate functions $P_n(c)$ defined in ref. 21. The details of this calculation can be found in ref. 22. The implication of these results is that dependence of the perturbative correction on the amount of magnetic TM ions being substituted into the semiconducting ZnO NPs will depend on whether net exchange interaction is ferromagnetic or antiferromagnetic. According to the increase in the

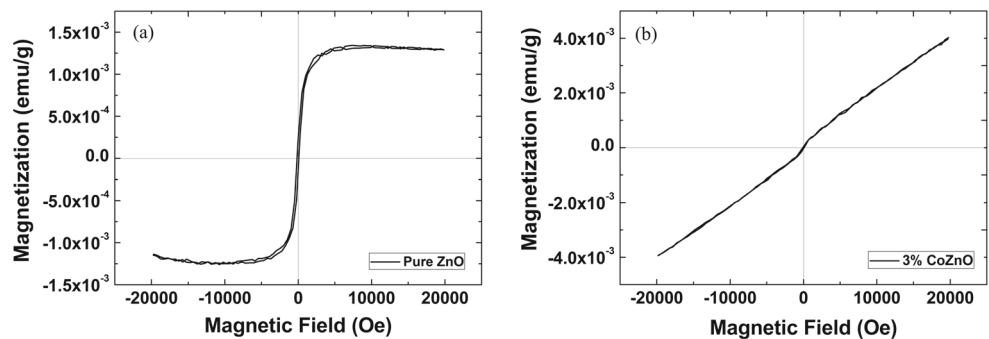
Table 4 Coercivity (H_c), saturation magnetization (M_s) of the Co-doped ZnO nanorods. The saturation magnetizations are expressed in units of μ_B /Co ions which allows for discussion of the competition between the direct and indirect exchange interactions which are present in the dilute magnetic semiconductor (DMS)

| Chemical formula | H_c (Oe) | M_s (emu/g) | M_s (μ_B /Co ²⁺ ions) |
|--|------------|---------------|---|
| ZnO | 118.152 | 0.001180 | – |
| Co _{0.009} Zn _{0.934} O _{1.057} | 107.411 | 0.000893 | 0.002095 |
| Co _{0.016} Zn _{0.714} O _{1.269} | 128.893 | 0.001983 | 0.002616 |
| Co _{0.036} Zn _{0.594} O _{1.370} | 85.929 | 0.003964 | 0.002324 |
| Co _{0.045} Zn _{0.634} O _{1.320} | 64.446 | 0.008009 | 0.003723 |
| Co _{0.051} Zn _{0.598} O _{1.351} | 91.299 | 0.011770 | 0.004834 |

saturation magnetization, as the concentration of Co²⁺ ions increases from 1.8 to 2.6%, it is due to the fact that the net exchange interaction (which also depends on c since the average distance of the two ions decreases as more Co²⁺ replaces the Zn²⁺ ions located in the wurtzite structure) is ferromagnetic, i.e., it dominated the direct Co-Co interaction. For the case of Mn²⁺ doping into ZnO, the net interaction is dominated by the indirect antiferromagnetic Mn-O-Mn interaction [11].

At this point, we would like to comment on the values of the saturation magnetization we found in this study. As we have pointed out in ref. 11, most results are expressed in terms of emu/g. The difficulty with this is that the contributions to the gram term comes from the Co, the Zn, and the O ions while the emu depends on the Co ions present (assuming that the Zn ions having no unpaired electrons are not magnetic). Mohamed Basith et al. [23] reported that the M_s of Co_xZn_{1-x}O ranged from 0.485×10^{-3} to 2.203 emu/g as x varied between 0.5% and 3.0% emu/g. Castro et al. [24] obtained a M_s of 0.025 emu/g for $x = 0.1$. Like us, Sharma et al. [25] gave their saturation magnetization in units of μ_B /Co ion. They reported a value of 0.061 μ_B /Co ion for a Co_{0.2}Zn_{0.98}O nanoparticle. This value is of the same order of magnitude as the values we found in other Co-doped ZnO nanoparticles.

Fig. 6 Magnetic hysteresis loops the pure ZnO and 3% Co-doped ZnO NRs. (a) Hysteresis loop of pure ZnO NRs. The diamagnetic contribution (extrapolation of the high field part of the loop) to the magnetization was subtracted from the loop. (b) Hysteresis loop of the 3% Co-doped ZnO NRs. The diamagnetic contributions were not subtracting from the loops for the Co-doped NRs



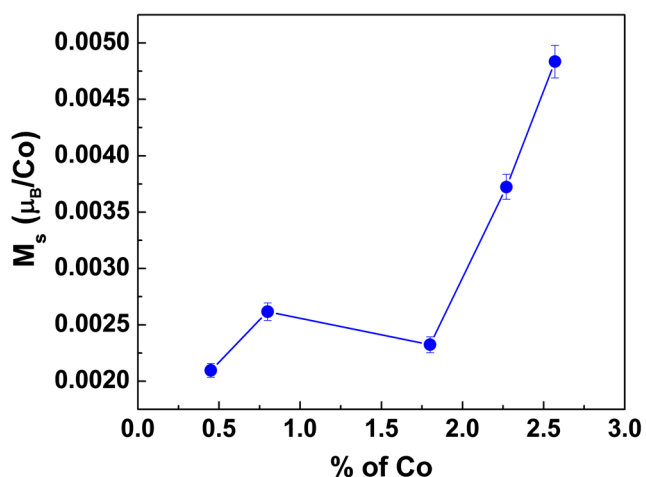


Fig. 7 Plot of the saturation magnetization (Bohr magneton/ Co^{2+} ions) vs. actual Co content. As we see, as the amount of Co increased from 1.8 to 2.2 to 2.5%; the saturation magnetization increased from 2.324 to 3.723 to $4.634 \times 10^{-3} \mu_B/\text{Co}$ ion as listed in Table 4

4 Conclusion

This study and that of ref. 11 have both looked at the effects of doping magnetic ions (Co and Mn) into ZnO NRs; doing so yields dilute magnetic semiconductors (DMS). We have performed similar measurements to characterize the two DMSs, $\text{Zn}_{1-x}\text{Co}_x\text{O}$, and $\text{Zn}_{1-x}\text{Mn}_x\text{O}$. Both of them form into the hexagonal wurtzite structure nanorods. The photoluminescence spectrums of both magnetic ion-doped ZnO NRs show that there is a high degree of defects in their structures. The magnetic properties of both series of magnetic ion-doped ZnO NRs are assumed to be determined by competing interactions (between direct TM-TM (ferromagnetic) interactions and indirect TM-O-TM (antiferromagnetic) interactions). In ref. 7, Coey et al. illustrated how the bound magnetic polarons are formed by two TM ions interacting with the shallow donor states at the oxygen vacancies. In their paper, Coey et al. presents an illustration of the band structure of an oxide with 3d impurities and a spin-split donor impurity band. The important thing to note is that an oxygen vacancy is needed in order for there to be a donor state.

The best way to monitor the presence of impurity defect oxide is photoluminescence studies since the PL spectrum provides information on the defects in the ZnO NPs. We have mentioned previously that the intensities of the 570 nm emission of the doped ZnO NPs decrease as the amount of Co replacing the Zn as the concentration of the Co replacement increases from 1.80 to 2.57%. The 560 nm emission in the PL spectrum occurs when an excited electron goes into the ground-state energy level of interstitial singly ionized O^- ion. This interstitial ion came from one of the oxygen sites in the wurtzite structure of ZnO NP, leaving behind a vacancy. A decrease of the intensities of the PL emission indicated that number of vacancies created had decreased. The decrease in

the number of vacancies could mean that there is lesser amount of antiferromagnetic contribution to the net exchange interaction (arising from the presence competing interactions between the TM ions in the TM-doped ZnO semiconductor). The replacement of more Zn by Co ions could mean that the average separation of the Co ions had increased. This will lead to an increase in the contribution of the ferromagnetic exchange interaction to the Co ions. The net exchange interaction would increase as more Co ions replaced the Zn ions in the DMS Co:ZnO NPs.

Funding Information This study was financially supported by the Royal Golden Jubilee Scholarship (The Thailand Research Fund) and the King Mongkut's University of Technology, Thonburi, through the KMUTT 55th Anniversary Commemorative Fund.

References

- Matthais, B.T., Bozorth, R.M., Van Vleck, J.H.: Ferromagnetic interaction in EuO. *Phys. Rev. Lett.* **7**(5), 160–161 (1961)
- Schmehl, A., Vaithyanathan, V., Hermberger, A., Thiel, S., Richter, C., Liberati, M., Heeg, T., Röckerath, M., Kourkoutis, L.F., Mühlbauer, S., Böni, P., Müller, D.A., Barash, Y., Schubert, J., Idzerda, Y., Mannhart, J., Schlom, D.G.: Epitaxial integration of the highly spin-polarized ferromagnetic semiconductor EuO with silicon and GaN. *Nat. Mater.* **6**, 882–887 (2007)
- Furdyna, J.K.: Diluted magnetic semiconductors. *J. Appl. Phys.* **64**, R29–R32 (1988). <https://doi.org/10.1063/1.341700>
- Ohno, D.: (Ga, Mn) As: a new diluted magnetic semiconductor based on GaAs. *Appl. Phys. Lett.* **69**, 363–365 (1996). <https://doi.org/10.1063/1.118061>
- Dietl, T., Ohno, H., Matsukura, F., Cibert, J., Ferrand, D.: Zener model description of ferromagnetism in zinc-blende magnetic semiconductors. *Science*. **287**, 1019–1022 (2000)
- Zener, C.: Interaction between the d shells in the transition metals. *Phys. Rev.* **81**(4), 440–444 (1950)
- Coey, J.M.D., Venkatesan, M., Fitzgerald, C.B.: Donor impurity band exchange in dilute ferromagnetic oxides. *Nat. Mater.* **4**(2), 173–179 (2005)
- Venkatesan, M., Fitzgerald, C.B., Lumney, J.G., Coey, J.M.D.: Anisotropic ferromagnetism in substituted zinc oxide. *Phys. Rev. Lett.* **17**, 1772061–1772064 (2004)
- Anghej, J., Thurber, A., Tenne, D.A., Hanna, C.B., Punnoosa, A.: Correlation between saturation magnetization, bandgap, and lattice volume of transition metal (M=Cr, Mn, Fe, Co, or Ni) doped $\text{Zn}_{1-x}\text{M}_x\text{O}$ nanoparticles. *J. Appl. Phys.* **107**, 09E3141–09E3143 (2010). <https://doi.org/10.1063/1.3360189>
- Durst, A.C., Bhatt, R.N., Wolff, P.A.: Bound magnetic polaron interactions in insulating doped diluted magnetic semiconductors. *Phys. Rev. B.* **65**, 2352051–23520510 (2002)
- Thongjamroon, S., Ding, J., Heng, T.S., Tang, I.M., Thongmee, S.: Dependence of the magnetic properties of the dilute magnetic semiconductor $\text{Zn}_{1-x}\text{Mn}_x\text{O}$ nanorods on their Mn doping levels. *JMMM*. **439**, 391–396 (2017)
- Ueda, K., Tabata, H., Kawai, T.: Magnetic and electric properties of transition-metal-doped ZnO films. *Appl. Phys. Lett.* **79**, 988–990 (2001). <https://doi.org/10.1063/1.1384478>
- Ney, A.: Element specific versus integral structural and magnetic properties of co:ZnO and Gd:GaN probed with hard X-ray absorption spectroscopy. *Materials*. **3**, 3565–3613 (2010)

14. Tietze, T., Gacic, M., Schütz, G., Jakob, G., Brück, S., Goering, E.: XMCD studies on Co and Li doped ZnO magnetic semiconductors. *New J. Phys.* **10**, 055009 (2008)
15. Martinez, B., Sandiumenge, F., Balcells, L., Arbiol, J., Sibieude, F., Monty, C.: Structure and magnetic properties of Co-doped ZnO nanoparticles. *Phys. Rev. B.* **72**, 1652021–1652028 (2005)
16. Balti, I., Mezni, A., Omrani, A.D., Leone, P., Viana, B., Brinza, O., Smiri, L.S., Jouini, N.: Comparative study of Ni- and Co-substituted ZnO nanoparticles: synthesis, optical, and magnetic properties. *J. Phys. Chem. C.* **115**, 15758–15766 (2011)
17. Franco Jr., A., Pessoni, H.V.S., Ribeiro, P.R.T., Machado, F.L.A.: Magnetic properties of Co-doped ZnO nanoparticles. *JMMM.* **426**, 347–350 (2017)
18. John Wiley & Sons: Introduction to solid state physics, 4th edition. In: USA (1971)
19. Djuricic, A.B., Choy, W.C.H., Roy, V.A.L., Leung, Y.H., Kwong, C.Y., Cheah, K.W., Gundu Rao, T.K., Chan, W.K., Fei Lui, H., Surya, C.: Photoluminescence and electron paramagnetic resonance of ZnO tetrapod structures. *Adv. Funct. Mater.* **14**, 856–864 (2004)
20. Tauc, J.: Optical properties and electronic structure of amorphous Ge and Si. *Mater. Res. Bull.* **3**, 37–46 (1968)
21. Edwards, S.F., Jones, R.C.: A green function theory of spin waves in randomly disordered systems. *J. Phys. C4*, 2109–2126 (1971)
22. Coey, J.M.D., Venkatesam, M., Fitzgerald, C.B.: Donor impurity band exchange in dilute ferromagnetic oxides. *Nat. Mater.* **4**(2), 173–179 (2005)
23. Mohamed Basith, N., Vijaya, J., Kennedy, L.J., Bououdina, M., Jenefer, S., Kaviyanasan, V.: Co-doped ZnO nanoparticles: structural, morphological, optical, magnetic and anti bacterial studies. *J. Nanosci. Technol.* **30**(11), 1108–1117 (2014)
24. Castro, T.J., Rodrigues, P.A.M., Oliveira, A.C., Franco Jr., A., Pessoni, H.V.S., Morais, P.C., de Silva, S.W.: Optical and magnetic properties of Co-doped ZnO nanoparticles and the onset of ferromagnetic order. *J. Appl. Phys.* **121**, 013904 (2014)
25. Sharma, V.K., Najm, M., Srivastava, A.K., Varma, G.D.: Structural and magnetic studies on transition metal (Mn, Co) doped ZnO nanoparticles. *JMMM.* **324**, 683–689 (2012)

Publisher's Note Springer Nature remains neutral with regard to jurisdictional claims in published maps and institutional affiliations.